Langmuir
Article
pubs.acs.org/Langmuir

Thin Film Assembly of Spider Silk-like Block Copolymers

Sreevidhya T. Krishnaji,[†,‡] Wenwen Huang,[§] Olena Rabotyagova,[†,‡] Eugenia Kharlampieva,[∥] Ikjun Choi,[∥] Vladimir V. Tsukruk,*[,∥] Rajesh Naik,[⊥] Peggy Cebe,[§] and David L. Kaplan*[,†,‡]

[†]*Department of Biomedical Engineering, Tufts University, 4 Colby Street, Medford, Massachusetts 02155, United States,* [‡]*Department of Chemistry, Tufts University, 62 Talbot Avenue, Medford, Massachusetts 02155, United States,* [§]*Department of Physics, Tufts University, 4 Colby Street, Medford, Massachusetts 02155, United States,* [∥]*Materials Science and Engineering, Georgia Institute of Technology, 771 Ferst Drive, N.W., Atlanta, Georgia 30332, United States, and* [⊥]*Air Force Research Laboratory, Materials and Manufacturing Directorate, Biotechnology Group, Wright-Patterson Air Force Base, Dayton, Ohio 45433, United States*

Received July 1, 2010. Revised Manuscript Received November 26, 2010

We report the self-assembly of monolayers of spider silk-like block copolymers. Langmuir isotherms were obtained for a series of bioengineered variants of the spider silks, and stable monolayers were generated. Langmuir−Blodgett films were prepared by transferring the monolayers onto silica substrates and were subsequently analyzed by atomic force microscopy (AFM). Static contact angle measurements were performed to characterize interactions across the interface (thin film, water, air), and molecular modeling was used to predict 3D conformation of spider silk-like block copolymers. The influence of molecular architecture and volume fraction of the proteins on the self-assembly process was assessed. At high surface pressure, spider silk-like block copolymers with minimal hydrophobic block (f_A = 12%) formed oblate structures, whereas block copolymer with a 6-fold larger hydrophobic domain (f_A = 46%) formed prolate structures. The varied morphologies obtained with increased hydrophobicity offer new options for biomaterials for coatings and related options. The design and use of bioengineered protein block copolymers assembled at air−water interfaces provides a promising approach to compare 2D microstructures and molecular architectures of these amphiphiles, leading to more rationale designs for a range of nanoengineered biomaterial needs as well as providing a basis of comparison to more traditional synthetic block copolymer systems.

The self-assembly of amphiphilic block copolymers provides a useful and versatile approach to pattering synthetic and biopolymer surfaces,[1] drug delivery, tissue engineering,[2] and diagnostics[3] as well as the formation of periodic structures at nanoscale.[4] Precise control of one block with respect to the other helps tune molecular architecture and tweak secondary structure, folding, vertical, and lateral segregation modes, and self-assembly. In addition to their behavior during conventional spin- or drop-casting, the Langmuir−Blodgett (LB) technique can be exploited to provide means for directed assembly of amphiphilic block copolymers. Controlled deposition of LB monolayers on solid substrates in different states allows characterizing the morphology and surface properties of block copolymers at air−water interfaces, with the structures formed dependent on various parameters including the relative compression, length of blocks, pH, temperature, and concentration.[5,6]

In contrast to the large literature of synthetic block copolymers assembled at air−water interfaces, natural polymers, such as proteins and polysaccharides, are under-studied. For example, the self-assembly process of block copolymers composed of poly(ethylene oxide) (PEO) and polystyrene (PS) are well studied. Two-dimensional aggregation of PEO−PS block copolymers[7] at air−water interfaces has been extensively explored, and the polymers were found to form surface aggregates with morphologies like dots, spagetti-like, network structures, planar continents, and chains, depending on the size, shape, symmetry, relative molecular weight of the blocks, and concentration. In contrast, limited study has been devoted to the thin film self-assembly of natural biopolymers.[8−11] There are many fibrous proteins in nature with repetitive sequences responsible for folding to structural elements and defined properties, including silks,[12,13]collagens,[14] elastin,[15] fibronectin,[16] and keratin.[17] Careful

*To whom correspondence should be addressed: e-mail david.kaplan@tufts.edu, Tel 617-627-3251, Fax 617-627-3231 (D.L.K.); e-mail vladimir@mse.gatech.edu, Tel 404-894-6081, Fax 404-894-9140 (V.V.T.).

(1) Gupta, M. K.; Singamaneni, S.; McConney, M.; Drummy, L. F.; Naik, R. R.; Tsukruk, V. V. *Adv. Mater*. **2010**, *22*, 115.
(2) Beattie, D.; Wong, K. H.; Williams, C.; Poole-Warren, L. A.; Davis, T. P.; Barner-Kowollik, C.; Stenzel, M. H. *Biomacromolecules* **2006**, *7*, 1072.
(3) Trubetskoy, V. S. *Adv. Drug Delivery Rev*. **1999**, *37*, 81.
(4) Grason, G. M. *Phys. Rep*. **2006**, *433*, 1.
(5) (a) Park, J. H.; Liu, N.; Mays, J.; Dadmun, M.; Advincula, R. *Soft Matter* **2009**, *5*, 747. (b) Seo, Y.; Cho, C. Y.; Hwangbo, M.; Choi, H. J.; Hong, S. M. *Langmuir* **2008**, *24*, 2381. (c) Azzam, T.; Eisenberg, A. *Angew. Chem., Int. Ed*. **2006**, *45*, 7443.
(6) Peleshanko, S.; Tsukruk, V. V. *Prog. Polym. Sci*. **2008**, *33*, 523.
(7) (a) Deschênes, L.; Bousmina, M.; Ritcey, A. M. *Langmuir* **2008**, *24*(8), 3699. (b) Cox, J. K.; Yu, K.; Constantine, B.; Eisenberg, A.; Lennox, R. B. *Langmuir* **1999**, *15*, 7714. (c) Pagac, E. S.; Prieve, D. C.; Solomentsev, Y.; Tilton, R. D. *Langmuir* **1997**, *13*, 2993. (d) Fauré, M. C.; Bassereau, P.; Carignano, M. A.; Szleifer, I.; Gallot, Y.; Andelman, E. D. *Eur. Phys. J. B* **1998**, *3*, 365. (e) Cox, J. K.; Yu, K.; Eisenberg, A.; Lennox, R. B. *Phys. Chem. Chem. Phys*. **1999**, *1*, 4417. (f) Fauré, M. C.; Bassereau, P.; Lee, L. T.; Menelle, A.; Lheveder, C. *Macromolecules* **1999**, *32*, 8538.
(8) Muller, W. S.; Samuelson, L. A.; Fossey, S. A.; Kaplan, D. L. *MRS Symp. Proc*. **1993**, *292*, 181.
(9) Muller, W. S.; Samuelson, L. A.; Fossey, S. A.; Kaplan, D. L. *Langmuir* **1993**, *9*, 1857.
(10) Valluzi, R.; Gido, S. P.; Zhang, W.; Muller, W. S.; Kaplan, D. L. *Macromolecules* **1996**, *29*, 8606.
(11) Valluzi, R.; Gido, S. P.; Zhang, W.; Muller, W. S.; Kaplan, D. L. *Int. J. Biol. Macromol*. **1999**, *24*, 237.
(12) (a) Kaplan, D. L.; Mello, C. M.; Arcidiacono, S.; Fossey, S.; Senecal, K.; Muller, W. In *Protein-Based Materials*; McGrath, K. P., Kaplan, D. L., Eds.; Birkhaeuser: Cambridge, MA, 1997; pp 103−131.(b) Hayashi, C. Y.; Shipley, N. H.; Lewis, R. V. *Int. J. Biol. Macromol*. **1999**, *24*, 271. (c) Thiel, B. L.; Guess, K. B.; Viney, C. *Biopolymers* **1997**, *41*, 703.
(13) *Silk Polymers: Materials Science and Biotechnology*; Kaplan, D., Adams, W. W., Farmer, B., Viney, C., Eds.; American Chemical Society: Washington, DC, 1994.
(14) (a) Shoulders, M. T.; Raines, R. T. *Annu. Rev. Biochem*. **2009**, *78*, 929. (b) Rabotyagova, O. S.; Cebe, P.; Kaplan, D. L. *Mater. Sci. Eng*. **2008**, *28*, 1420.
(15) Urry, D. W. *J. Protein Chem*. **1988**, *7*, 1.
(16) Parry, D. A. D.; Fraser, R. D. B.; Squire, J. M. *J. Struct. Biol*. **2008**, *163*, 258.

observation of sequences in these proteins reveals similarities within these complex fibrous proteins and synthetic block copolymers.[18] Yet comparisons between the two sources of block copolymers is not available, where more subtle interactions in amino acid side chain chemistries would presumably lead to more complex interactions and thus confound previously reported morphologies generated from the synthetic systems such as PEO−PS.

Silk fibers obtained from silkworms and spiders are considered the strongest materials found in nature and are explored as components for high-performance composites.[19−23] These biomaterials have already been explored as matrices for high-performance nanocomposites with advanced mechanical properties.[24] Crystalline β-sheet regions of silk are observed due to the presence of GAGAS repeats in the silkworm, *Bombyx mori*,[13] and polyalanine (A_n) repeats in the spider *Nephila clavipes*,[12] with less crystalline domains segregating these regions to form the blocky structures. Orb weaving spiders, in particular *N. clavipes*, are commonly investigated and provide a benchmark for the study of silk fibers.[25,26] Spider silk fibers are composed of a mixture of two major proteins, MaSp1 and MaSp2 (MaSp: major ampullate spidroin). While both proteins have glycine- and alanine-rich residues with hard polyalanine regions (GA_n/A_n) responsible for β-sheet (crystalline structure) formation, some distinctions include MaSp1 with a soft stretch of tripeptide repeats (GGX, X = L, Q, R, Y), whereas MaSp2 has pentapeptide repeats (GPGQQ and GPGGY). In prior studies, we prepared stable LB films from native *B. mori* silk,[8,9,27] and more recently, monolayers have been reported from recombinant *N. clavipes* MaSp1 and MaSp2.[28] The differences in self-assembly of MaSp1 and MaSp2 in forming heterogeneous and homogeneous elastic films, respectively, were due to the presence of proline and slower aggregation for the latter protein.

We have previously reported the synthesis, purification, and assembly of a new family of spider silk-like block copolymers.[29,30] The current goal of the study was to exploit the amphiphilic and block-like nature of spider silks to determine assembled morphologies with varying lengths of hydrophobic blocks based on fundamental block copolymer theories.[31] The nature of immiscibility of block copolymers was used as a handle for preparing films one molecule thick at the air−water interface in the present study. The solution behavior of synthetic block copolymers that form micelles or aggregates has been studied in detail to understand how molecular properties allow formation and emergent properties of block copolymer vesicles.[32] The spider silk-like block copolymers were previously analyzed by attenuated total reflectance Fourier transform infrared spectroscopy (ATR-FTIR) in the solid state and by drop-casting from either water or 2-propanol for scanning electron microscopy (SEM).[29,30] It was observed that crystallinity increased as the number of polyalanine repeats increased and morphologies like spheres, rod-like, bowl-shaped, and large compound micelles were formed depending on the block sequence and solution conditions used to self-assemble the proteins. The focus in the present work was on the use of 2D thin film assemblies to further probe relationships between spider silk-like block copolymer sequences and morphological features of the assembled material systems.

The objective of the present study was to characterize this novel class of bioengineered spider silk-like block copolymers upon assembly at the air−water interface, as a route to gain insight into the assembled structures, packing of the chains and ultimately leading to better insight into the relationships between protein amphiphilic sequence chemistry and material morphology. Increasing the volume fraction of one of the spider silk-like blocks (in this case the hydrophobic block, block A) provided a handle with which to study the impact of sequence chemistry and block length on assembled morphology. To better understand the assembly mechanism and properties of these proteins, the adsorption behavior at the air−water interface was studied using surface pressure isotherms, ellipsometry, contact angle and atomic force microscopy (AFM).

Experimental Section

Materials. The spider silk-like block copolymers were synthesized by recombinant DNA technology as we have previously reported.[29] Briefly, a linker was inserted into pET 30a(+) (Novagen, Madison, WI) plasmid to introduce *NheI* and *SpeI* restriction sites, needed for subsequent cloning and development of multimers. Two spider silk modules block A and block B, derived from *Nephila clavipes* major ampullate 1 (MaSp1), were back-translated to DNA sequences based on optimal bacteria codon usage. Spider silk block sequences were prepared as oligomers and annealed to form double-stranded DNA. They were later digested with *NheI* and *SpeI* and ligated into modified pET 30a(+) plasmid. Stepwise ligations of block A lead to various constructs. After confirming inserts by DNA sequencing, they were expressed in *E. coli* RY-3041 strain, a mutant strain of *E. coli* BLR (DE3) deficient in the expression of of SlyD protein.[33] Cells were grown at 37 °C in LB medium and induced at OD_{600} 0.6 with 1 mM IPTG (isopropyl β-D-thiogalactoside) (Fisher Scientific, Hampton, NH) and harvested after 4 h. Purification of proteins was performed under denaturing conditions using Ni-NTA resin (Qiagen, Valencia, CA) using manufacturer's protocol.

Langmuir Studies. Langmuir isotherms at the air−water interface and LB deposition onto silicon substrates were performed at room temperature using a KSV 2000 LB mini-trough. The spider silk-like protein block copolymers were dissolved in hexafluoroisopropanol (HFIP) at a concentration 2 mg/mL and later diluted to different concentrations (HBA: 0.024 mg/mL; HBA_2: 0.5 mg/mL; HBA_6: 1 mg/mL) with chloroform (HPLC grade). Silicon wafers (Semiconductor Processing Co. Boston, MA) used for deposition of LB films were cleaned as follows. The preparation allowed for wafer decontamination of both organic and inorganic substances. The silicon wafers were cut into rectangular pieces (1.5 × 3.0 cm) and submerged in water (Nanopure, 18.2 MΩ cm), sonicated at room temperature for

(17) Fraser, R. D. B.; MacRae, T. P. *Conformation in Fibrous Proteins and Related Synthetic Polypeptides*; Academic Press: New York, 1973.
(18) Borner, H. G.; Schlaad, H. *Soft Matter* **2007**, *3*, 394.
(19) Lefevre, T.; Rousseau, M.-E.; Pezolet, M. *Biophys. J.* **2007**, *92*, 2885.
(20) Shao, Z.; Vollrath, F. *Nature* **2002**, *418*, 741.
(21) Altman, G. H.; Diaz, F.; Jakuba, C.; Calabro, T.; Horan, R. L.; Chen, J.; Lu, H.; Richmond, J.; Kaplan, D. L. *Biomaterials* **2004**, *24*, 401.
(22) Gosline, J. M.; Guerette, P. A.; Ortlepp, C. S.; Savage, K. N. *J. Exp. Biol.* **1999**, *202*, 3295.
(23) Hu, X.; Vasanthavada, K.; Kohler, K.; McNary, S.; Moore, A. M. F.; Vierra, C. A. *Cell. Mol. Life Sci.* **2006**, *63*, 1986.
(24) (a) Jiang, C.; Wang, X.; Gunawidjaja, R.; Lin, Y.-H.; Gupta, M. K.; Kaplan, D. L.; Naik, R. R.; Tsukruk, V. V. *Adv. Funct. Mater.* **2007**, *17*, 2229. (b) Kharlampieva, E.; Kozlovskaya, V.; Gunawidjaja, R.; Shevchenko, V. V.; Vaia, R.; Naik, R. R.; Kaplan, D. L.; Tsukruk, V. V. *Adv. Funct. Mater.* **2010**, *20*, 840–846.
(25) Xu, M.; Lewis, R. V. *Proc. Natl. Acad. Sci. U.S.A.* **1990**, *87*, 7120.
(26) Hinman, M. B.; Lewis, R. V. *J. Biol. Chem.* **1992**, *267*, 19320.
(27) Zhang, W.; Gido, S. P.; Muller, W. S.; Fossey, S. A.; Kaplan, D. L. *Proc. 51st Annu. Meet. Microsc. Soc. Am.* **1993**, 1216.
(28) Renault, A.; Dubé, J. F.; Lefèvre, T.; Pezennec, S.; Beaufils, S.; Vié, V.; Tremblay, M.; Pézolet, M. *Langmuir* **2009**, *25*, 8170.
(29) Rabotyagova, O. S.; Cebe, P.; Kaplan, D. L. *Biomacromolecules* **2009**, *10*, 229.
(30) Rabotyagova, O. S.; Cebe, P.; Kaplan, D. L. *Macromol. Biosci.* **2010**, *10*, 49.
(31) (a) Hamley, J. W. *The Physics of Block Copolymers*; Oxford University Press: Oxford, 1998.(b) Castello, V.; Hamley, I. W. *Curr. Opin. Solid State Mater. Sci.* **2004**, *8*, 426. (c) Hamley, I. W. *Prog. Polym. Sci.* **2009**, *34*, 1161.
(32) J Discher, D. E.; Eisenberg, A. *Science* **2002**, *297*, 967.
(33) Bini, E.; Foo, C. W. P.; Huang, J.; Karageorgiou, V.; Kitchel, B.; Kaplan, D. L. *Biomacromolecules* **2006**, *7*, 3139.

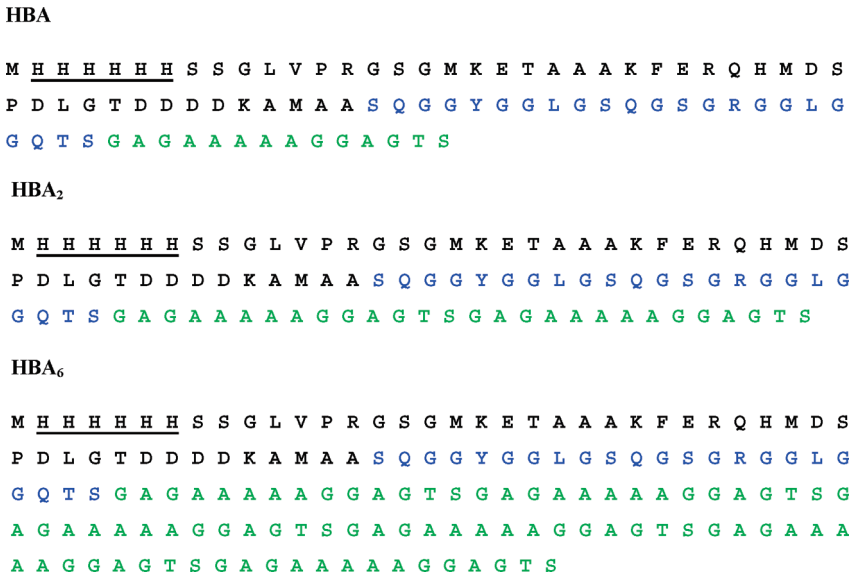

Figure 1. Amino acid sequence of genetically engineered spider silk-like block copolymers. Histidine tag is underlined. Blocks B and A are represented by blue and green colors, respectively.

10 min, and treated with piranha solution (30% hydrogen peroxide, 70% concentrated sulfuric acid) for 1 h. The substrates were then rinsed with Nanopure water and dried with a nitrogen stream. The substrates were prepared in a clean room environment. The mini-trough was filled with Nanopure water, and the block copolymer solution was then deposited in several droplets (60−80 μL) on to water subphase and subsequently left to stand for 30 min to allow complete evaporation of chloroform. The monolayers were then compressed at a rate of 5 mm/min before deposition and films deposited at a rate of 2 mm/min. The cross-sectional area in the condensed state, A_0, was derived from pressure−area isotherms by using the tangent line corresponding to the first steep rise in the surface pressure.[34] During LB deposition, the surface pressure was held constant as the submerged substrate was lifted slowly at the rate of 2 mm/min.

Characterization of the Films. Surface morphology of Langmuir monolayer was studied in the light tapping mode using a Dimension 3000 Nanoscope IIIa (Digital Instruments, Woodbury, NY) with silicon tips in according to procedure adapted in our studies.[35] Deposited monolayers were dried completely overnight, with images taken at three different regions for consistency, and flattened and plane-fitted as required. The thickness of films was measured by M2000U Woolam spectroscopic ellipsometer (J.A. Woollam Co., Inc., Lincoln, NE) by adjusting three angles at 60°, 65°, and 70°.

Contact Angle. Water contact angles were measured on monolayer films prepared using the LB technique by means of contact angle goniometer (KSV). Contact angle (CA) was measured by adding a drop of water until the largest contact angle was achieved without increasing the solid/liquid interfacial area. CA values of the right side and the left side were measured, and an average value was used. All CA data were an average of at least three measurements on different locations of the film.

Dynamic Light Scattering. DLS experiments were performed using a Brookhaven Instrument BI200-SM goniometer (Holtsville, NY) equipped with a diode laser operated at a wavelength, $\lambda = 532$ nm. All samples were prepared in a similar way to those prepared for LB studies and were filtered through a low protein binding, 5 μm membrane (Millex-SV, Millipore, Billerica, MA) prior to DLS measurements. The temperature was kept at 25 °C with 0.05 °C accuracy with a temperature-controlled recirculating bath. The corresponding particle size distributions were obtained using the CONTIN method.

Molecular Modeling. Prediction of 3D structure of model proteins HBA and HBA_6 were obtained by performing simulations on Materials Studio (V3.1) software from Accelrys simulation program. Each of the amino acid sequences was built, and their geometries were optimized through the energy minimization tool in the Discover module using the PCFF force field and the Smart Minimizer. The simulation procedure involved (i) constructing amino acid structures using Visualizer module, a sketching tool in Materials Studio, (ii) optimizing the structures using PCFF force field and Smart minimize tool in Discovery module, and (iii) optimizing geometry with minimize tool in Discover module.

Results and Discussion

Figure 1 provides the amino acid sequences of the spider silk-like block designs used in the present study. Block A (GAGAAAAAGGAG) comprised poly alanine/glycine repeats that forms β-sheets[36,37] and is designated as the hydrophobic block (colored green). Block B is composed of less crystalline glycine rich regions, GGX (where X = tyrosine, leucine, glutamine) that contribute to elasticity[38,39] and is hydrophilic (colored blue). The presence of serine and arginine helps in the formation of hydrogen bonds. The H block includes a hexahistidine (his tag, underlined) useful for purification along with a linker sequence. The spider silk-like block copolymer constructs in consideration are designated as follows with molecular weight (Da) in parentheses: HBA (8127 Da), HBA_2 (9097 Da), and HBA_6 (12 981 Da).

The influence of histidine purification tags on genetically engineered proteins is important but rarely studied.[40−42]

(34) Small, D. M. *The Physical Chemistry of Lipids*; Plenum Press: New York, 1986.
(35) (a) Tsukruk, V. V. *Rubber Chem. Technol.* **1997**, *70*, 430.(b) McConney, M. E.; Singamaneni, S.; Tsukruk, V. V. *Polym. Rev.* **2010**, in press.
(36) Simmons, A. H.; Ray, E. D.; Jelinski, L. W. *Macromolecules* **1994**, *27*, 5235.
(37) Liivak, O.; Flores, A.; Lewis, R.; Jelinski, L. *Macromolecules* **1997**, *30*, 7127.
(38) van Beek, J. D.; Hess, S.; Vollrath, F.; Meier, B. H. *Proc. Natl. Acad. Sci. U.S.A.* **2002**, *99*, 10266.
(39) Holland, G. P.; Creager, M. S.; Jenkins, J. E.; Lewis, R. L.; Yarger, J. L. *J. Am. Chem. Soc.* **2008**, *130*, 9871.
(40) Farmer, R. S.; Argust, L. M.; Sharp, J. D.; Kiick, K. L. *Biomacromolecules* **2006**, *39*, 162.
(41) Sharma, N.; Top, A.; Kiick, K. L.; Pochan, D. J. *Angew. Chem., Int. Ed.* **2009**, *48*, 7078.
(42) Xu, C.; Kopececk, J. *Pharm. Res.* **2008**, *3*, 674.

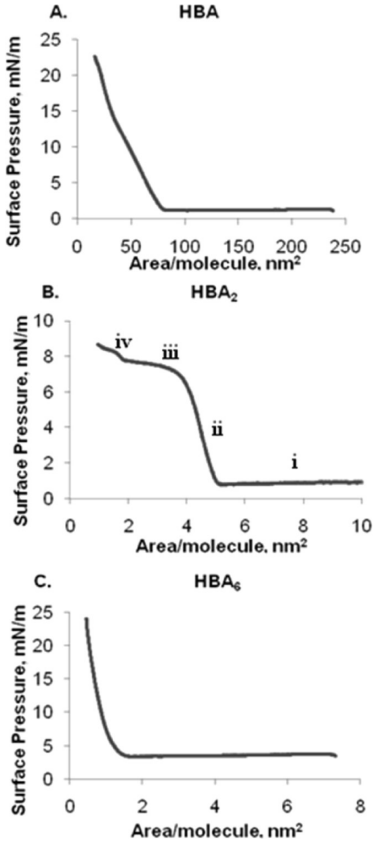

Figure 2. Pressure−area ($\pi-A$) isotherms for spider silk block copolymers HBA (A), HBA_2 (B), and HBA_6 (C). (B) Various regions of HBA_2: i, gas phase; ii, liquid extended phase; iii, plateau region; iv, liquid condensed phase.

Alanine-rich helical peptides[40] were purified with the help of a decahistidine fusion tag, and gold nanoparticle arrays prepared with the protein[41] allowed self-assembly along the fibril length where histidine segments played an important role in templating. The influence of linker sequences and histidine fusion tag on the self-assembly of block copolymer hydrogels (polyelectrolyte and coiled coil segments)[42] was not clearly explained. Physicochemical properties of stimuli responsive hybrid hydrogels mixed with Ni^{2+}/chelating ligands have been analyzed,[43] and the immobilization of histidine fusion proteins with lipids/chelating agents like Ni^{2+} at air−water and air−solid interfaces is useful for structural biology applications.[44,45] Pressure−area isotherms showed that the presence of Cu^{2+} at the air−water interface was responsible for enhancing the rate and extent of myoglobin binding on Cu^{2+}:IDA (IDA: imino diacetate) lipid monolayer films.[46]

In the present study, the fusion tag and the hydrophilic block length remain constant throughout for all samples, which allowed us to focus on the self-assembly of the block copolymers at the air−water interface. Further, in our prior studies,[29] distinct morphologies of genetically engineered and synthetically prepared spider silk-like block copolymer system was studied with/without the histidine fusion, respectively, corroborating the fusion partner to be less influential in self-assembly at least for larger proteins,[47] as in HBA_2 and HBA_6.

(43) Wang, C.; Stewart, R. J.; Kopecek, J. *Nature* **1999**, *397*, 417.
(44) Thompson, D. H.; Zhou, M.; Grey, J.; Kim, H. K. *Chem. Lett.* **2007**, *8*, 956.
(45) Kim, Y. S.; Chase, B.; Kiick, K. L.; Rabolt, J. F. *Langmuir* **2009**, *26*, 336.
(46) Shnek, D. R.; Pack, D. W.; Sasaki, D. Y.; Arnold, F. H. *Langmuir* **1994**, *10*, 2382.
(47) Goeden-Wood, N. L.; Keasling, J. D.; Muller, S. J. *Macromolecules* **2003**, *36*, 2932.

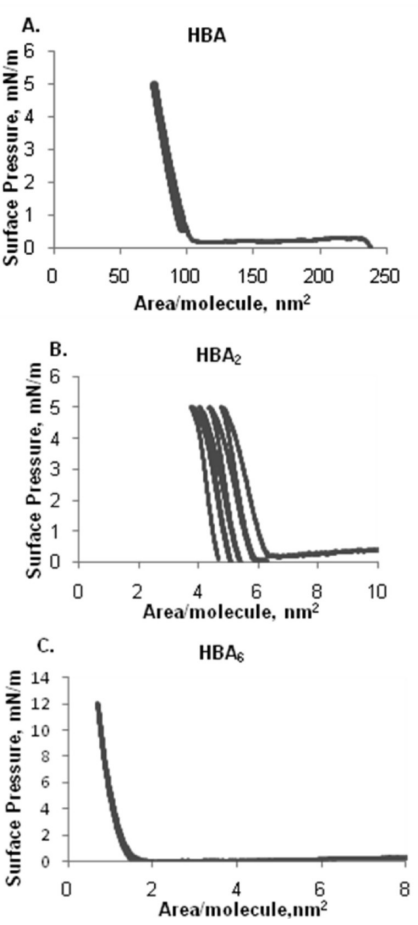

Figure 3. Compression−decompression cycles of HBA (A), HBA_2 (B), and HBA_6 (C).

Interfacial Assembly. In an earlier study, we showed stable monolayer silk films[9] could be generated from silkworm silk at an air−water interface. ATR-FTIR indicated these assemblies were β-sheets (silk II polymorph). In other studies, a new polymorph of *Bombyx mori* fibroin was found with a trigonal unit cell and a hexagonal packing of the chains, similar to polyglycine II.[11,12] The spider silk-like block copolymers formed stable Langmuir monolayers as indicated by pressure−area ($\pi-A$) isotherms. The block copolymers spread efficiently to form monolayers and did not dissolve in the water subphase, as indicated from Figure 2. The reversibility of Langmuir monolayers was examined by repeating the compression−decompression cycles at a lower pressure (5 mN/m). The isotherms were reversible upon multiple compression−decompression cycles (Figure 3); no significant hysteresis was observed for HBA and HBA_6, indicating that the proteins did not dissolve in water and also that the film elastically corresponded to changes in area. The pressure−area isotherms indicate that the amphiphilic block copolymers possess an appropriate balance in order to form stable monolayer films. The conformation adopted by protein at the air−water interface is complex due to the loss of free energy of the system. The composition of different hydrophobic block lengths determined the molecular packing and monolayer stability at the air−water interface, based on the differences in the pressure−area isotherms, area per molecule, and collapse of the monolayers for the various proteins as will be discussed below (Figures 2 and 3).

Stability and Reversibility. $\pi-A$ isotherms of the constructs are depicted in Figure 2. Surface compression behavior depends on the number of hydrophobic repeats. As the number of

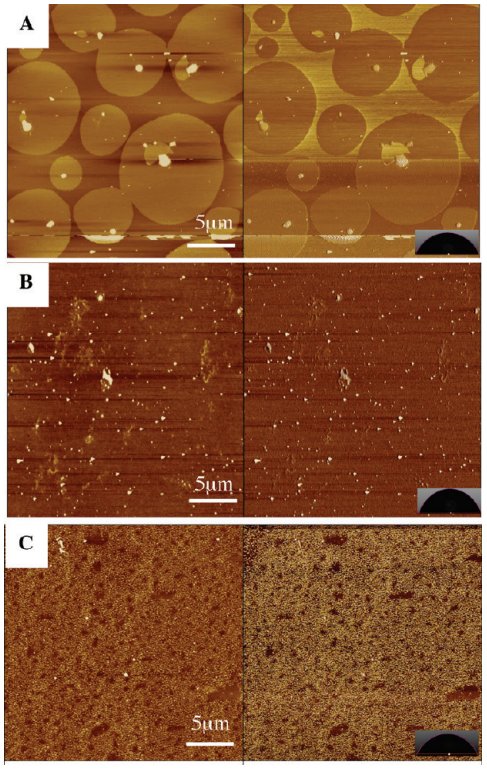

Figure 4. Topographical (left) and phase (right) AFM images of monolayers of spider silk-like block copolymers HBA (A), HBA_2 (B), and HBA_6 (C) at high surface pressure (8 mN/m). *Z*-scale for topography is 10 nm (b, c) and 20 nm (a); *z*-scale for phase is 20° (a, c) and 10° (b). Inset shows contact angle as measured.

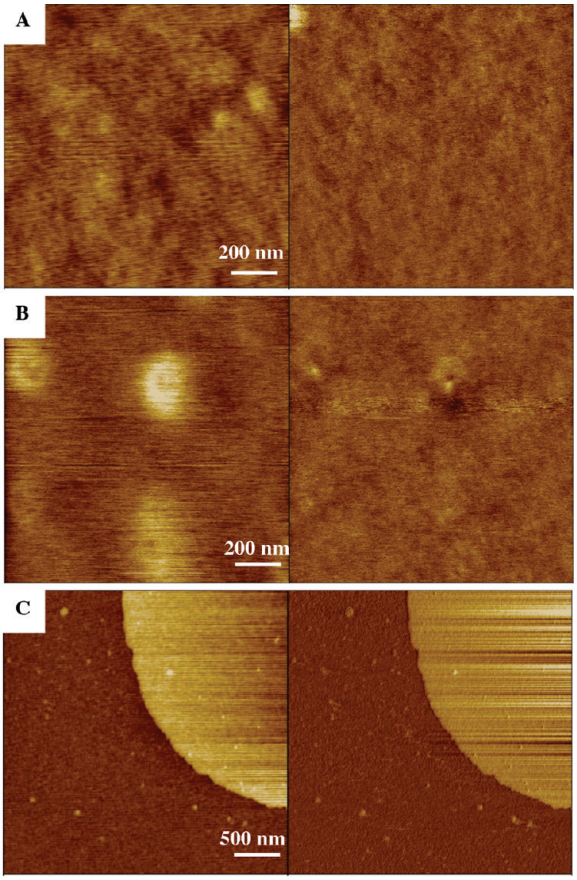

Figure 5. Monolayers of HBA prepared at low, medium, and high surface pressures (1, 4, and 8 mN/m for A, B, and C, respectively). Topographical (left) and phase (right) *z*-scales are 3 nm and 3° (A, B), and 5 nm and 5° (C).

hydrophobic repeats increased, the surface area occupied by the molecules decreased. HBA, with the lowest fraction of hydrophobic content, occupied a larger molecular area when compared to HBA_6, which had the highest hydrophobic block content. This can be explained as follows: as the rigidity of the molecule increases, reflected in the increase in the A block, the chains achieve a more ordered arrangement or structured packing. This is a common behavior for synthetic amphiphilic block copolymers.[6]

The reversibility of the assemblies at the interface was studied by four cycles of compression−decompression cycles (Figure 3). Monolayer reversibility provides information about intermolecular interactions and elasticity. Several mechanisms for monolayer reversibility−irreversibility have been reported, including dissolution of the sample into the water subphase, monolayer cracking for brittle monolayers, and monolayer buckling for ductile monolayers.[48] Monolayer dissolution and cracking were irreversible, such that collapsed materials did not incorporate into monolayers upon expansion of films. Negligible hysteresis (< 10% surface area) was observed for HBA and HBA_6. However, it is worth noting that for HBA_2 the entire isotherm can be divided into four regions (Figure 2b): (i) gas state at $\pi = 0$ mN/m, (ii) extended liquid state, (iii) plateau region at $\pi = 7$ mN/m, and (iv) condensed-state region. As the monolayer is compressed into the liquid-expanded (LE) phase, the hydrophobic parts of the molecules contact each other and lift from the water surface but remain largely disordered and fluid. Further compression leads to a first-order transition to the liquid-condensed (LC) phase, marked by a plateau in the isotherm corresponding to LE and LC coexistence. Pronounced hysteresis was observed during compression−decompression cycles, which may have caused rearrangement of hydrophilic block from the water subphase (partial submergence into water subphase), and upon release of the surface pressure, they must overcome the energy barrier to become adsorbed again on the water surface. We did not observe an S phase in these studies.

Monolayer Organization on Solid Surfaces. AFM was employed to view selected surface morphologies of HBA, HBA_2, and HBA_6 (Figures 5, 6, and 7) deposited on silicon substrates at low (1 mN/m), intermediate (4 mN/m), and high (8 mN/m) surface pressures (SP). Topographical and phase images showed varied morphologies at various surfaces pressures. Figures 5c, 6c, and 7c and Scheme 2 indicate aggregation at higher pressure as the number of hydrophobic blocks increased. There are two approaches to understand the morphologies obtained: (i) how the molecules orient themselves at the air−water interface when the monolayer is deposited at different pressures and (ii) the effect of how the morphologies vary with increasing block length at a given surface pressure (e.g., 8 mN/m in this case).

At high surface pressure (Figure 4), increasing the block length of polyalanine repeats led to organized features. The formation of amphiphilic monolayers at the air−water interface is complicated, since it requires the reduction of entropy at the interface. HBA, with the fewest alanine repeats, formed loosely packed domains (lower aggregation number, i.e., number of molecules per domain) when compared to HBA_2; HBA_6 forms a densely packed film on the silicon surface because the formation of a relatively ordered structure can be achieved by the increased

(48) Yee, K.; Lee, C. *Annu. Phys. Chem.* **2008**, *59*, 771.

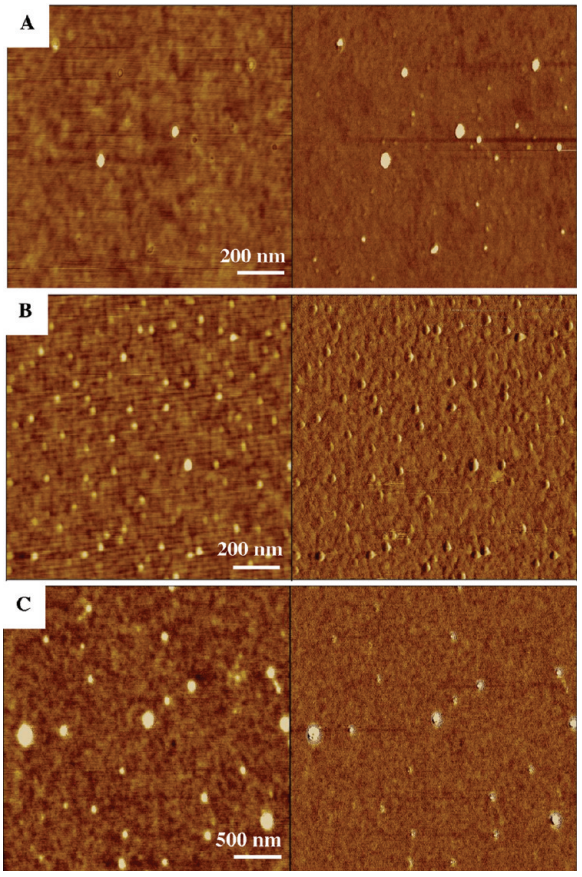

Figure 6. Monolayers of HBA_2 prepared at low, medium, and high surface pressures (1, 4, and 8 mN/m for A, B, and C, respectively). Topographical (left) and phase (right) *z*-scales are 3 nm and 5° for all images.

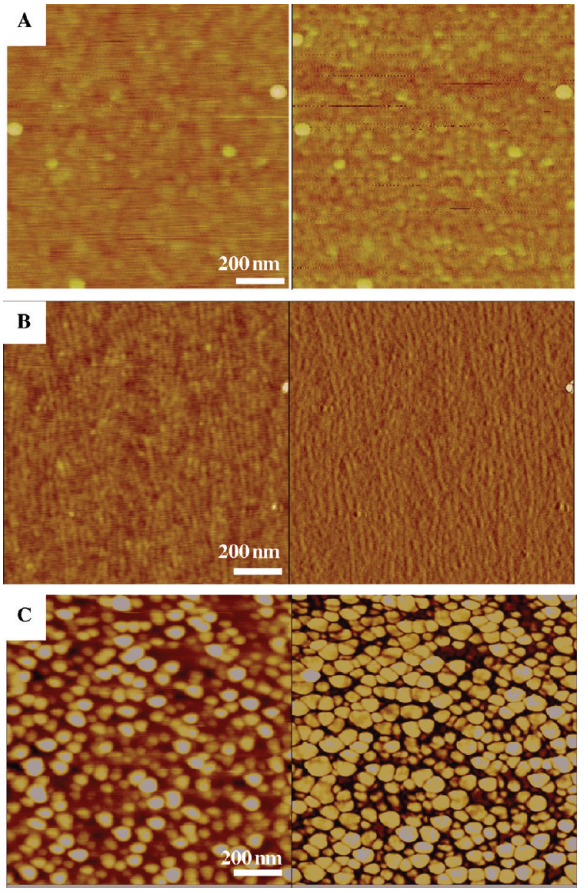

Figure 7. Monolayers of HBA_6 prepared at low, medium, and high surface pressures (1, 4, and 8 mN/m for A, B, and C, respectively). Topographical (left) and phase (right) *z*-scales are 3 nm and 5° (A), 3 nm and 3° (B), and 5 nm and 20° (C).

volume fraction of block A. Thus, with increased hydrophobic blocks, the morphologies change from the isolated features of HBA to closely packed circular domains with higher aggregation number with increased hydrophobic blocks. Although both surface energy and surface roughness are the dominant factors for wettability of materials, surface roughness[49] is the key factor once the components of the materials are selected. Contact angles were therefore measured for the samples at higher pressure. According to theory,[50] contact angles should be higher for the most hydrophobic samples[51] as the addition of a water droplet to the substrate decrease surface tension, minimizing interfacial area. This trend was observed from HBA to HBA_2, but contact angle decreased for HBA_6. Surface roughness of HBA_6 was ~1 nm. The decreased contact angle between the water droplet and the closely packed domains of HBA_6 may be due to partial transfer of the film onto the hydrophilic substrate.

The construct HBA at lower surface pressure (Figure 5A, monolayer deposited just before the pressure increases) exhibited a smooth thin film texture. As the pressure increased, the hydrophobic blocks segregated from the hydrophilic regions, observed as smaller emerging discs (Figure 5B) from the surface of the substrate. Higher surface pressures indicated the formation of loosely packed circular domains that were spread apart with diameters from 4 to 8 μm (Figure 5C). These domains were about 2.1 nm higher than the surrounding region and had a smooth layer at higher magnification with roughness less than 0.5 nm. Figure 6 indicates HBA_2 monolayer formed smooth textured films as pressure increased. HBA_6 formed an even monolayer with uniformly spread circular discs (mean diameter = 50 ± 6 nm) that appeared at low surface pressure (Figure 7A). Visible stripe-like structures were obtained at medium pressure. The enthalpy gain achieved by this reorganization balanced the loss of entropy caused by compression (Figure 7B). However, increasing the surface pressure caused a collapse of these string domains to circular domains, in contrast to stability of cylinders.[52] HBA_6, in contrast, was composed of circular domains at higher surface pressure that yielded densely packed structures. The diameter of the uniform circular domains (53 ± 8 nm) remained relatively constant over the area.

Table 1. Data Derived from Langmuir Isotherms and Contact Angles[a]

	thickness of monolayer,[b] nm			
protein	ellipsometry	atomic force microscopy	A_0, nm^2	contact angle at P_3 (deg)
HBA	2.7 ± 0.3	2.1 ± 0.4	83.7	50.3 ± 0.3
HBA_2	1.8 ± 0.2	1.9 ± 0.3	5.2	70.9 ± 0.8
HBA_6	1.3 ± 0.2	2.9 ± 0.6	1.3	51.3 ± 2.1

[a] A_0 is the mean molecular area/nm^2. P_3: contact angles measured at higher surface pressure (8 mN/m). [b] Thickness of monolayers from ellipsometer and AFM were obtained from three different regions.

(49) Wenzel, R. N. *J. Phys. Colloid Chem.* **1949**, *53*, 1466.
(50) Wenzel, R. N. *Ind. Eng. Chem.* **1936**, *28*, 988.
(51) Zhang, J.; Han, Y. *Langmuir* **2008**, *24*, 796.
(52) Israelachvili, J. N. *Intermolecular and Surface Forces*, 2nd ed.; Academic Press: San Diego, 1992.

Scheme 1. Proposed Model (Top View) To Explain Molecular Ordering in LB Monolayers from Spider Silk-like Block Copolymers at Different Surface Pressures[a]

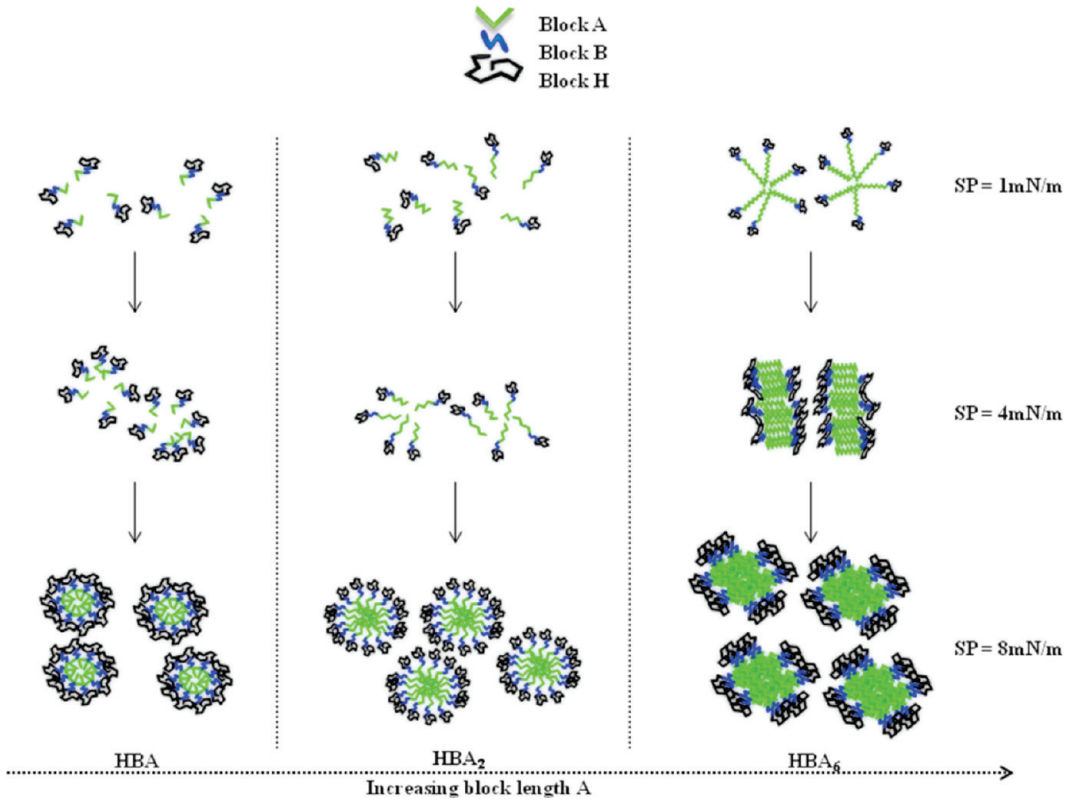

[a] SP = surface pressure, A block = hydrophobic, and B block = hydrophilic. Note: images are not to scale.

We found that the monolayer thickness measured by ellipsometry decreased as hydrophobicity increased at higher surface pressures (Table 1). A comparison of images showed that HBA adopted oblate or squashed structures, whereas HBA_6 adopted cylindrical or prolate shapes. The prolate structure for HBA_6 may be the result of hydrophobic−hydrophilic phase separation. The reduced height in HBA_6 was probably due to the propensity of the hydrophobic blocks coming close to one another to form β-sheets. Validation of crystallinity of HBA_6 has already been determined by FTIR and WAXS.[29,30] For HBA, during compression, we might suggest that the vertically aligned hydrophobic tail was mixed with the hydrophilic groups. Steric repulsion due to hydrophobic−hydrophilic interactions prevented dense packing and resulted in lower compressibility and hence oblate shapes and a larger area per molecule. HBA_2, more hydrophobic to HBA, preferred a more ordered circular domain. The differences in heights determined by AFM and ellipsometry may be due to (i) only partial transfer of the film to hydrophilic substrate (due to crystallinity of HBA_6) or (ii) regions where ellipsometric heights were obtained did not have complete transfer of the film.

Dynamic light scattering was used to determine whether micelles were formed in the bulk solution before addition to LB trough. The effective diameters of the assembled structures were different from that of the average diameter of the domains formed on the monolayers (HBA = 3.3 nm, HBA_2 = 143.3 nm, HBA_6 = 674.6 nm), indicating they are formed during monolayer assembly but not from bulk solution.

Model. Combining the different morphologies obtained by AFM, a model can be proposed for the spider silk-like block copolymers (Scheme 1). At lower surface pressure, molecules are at their most stable thermodynamic state. Less crystalline domains (block B) anchor in the water subphase, allowing the crystalline domains to form stable films at the interface for some

Scheme 2. Model (Side View) of the Role of Block A in Domain Size and Separation for Spider Silk-like Block Copolymers at Higher Surface Pressure[a]

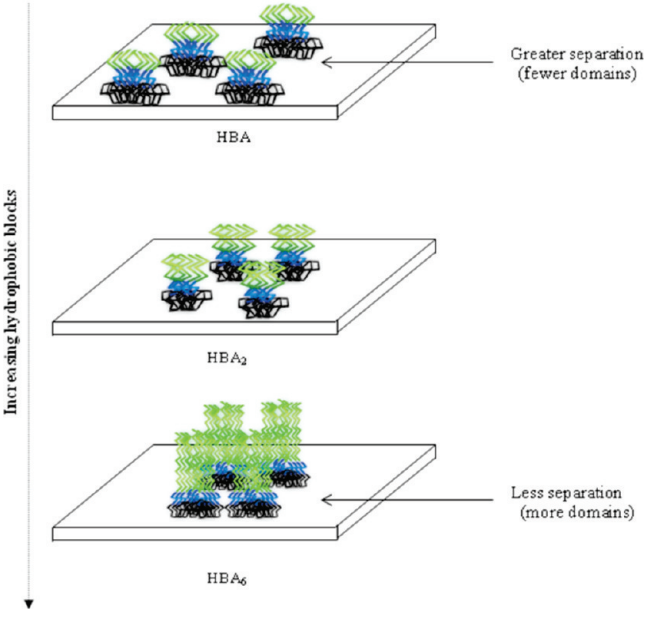

[a] As the number of repeats of block A increases, they tend to be nearer to each other, resulting in smaller domains. Blue represents hydrophilic blocks; green represents hydrophobic blocks.

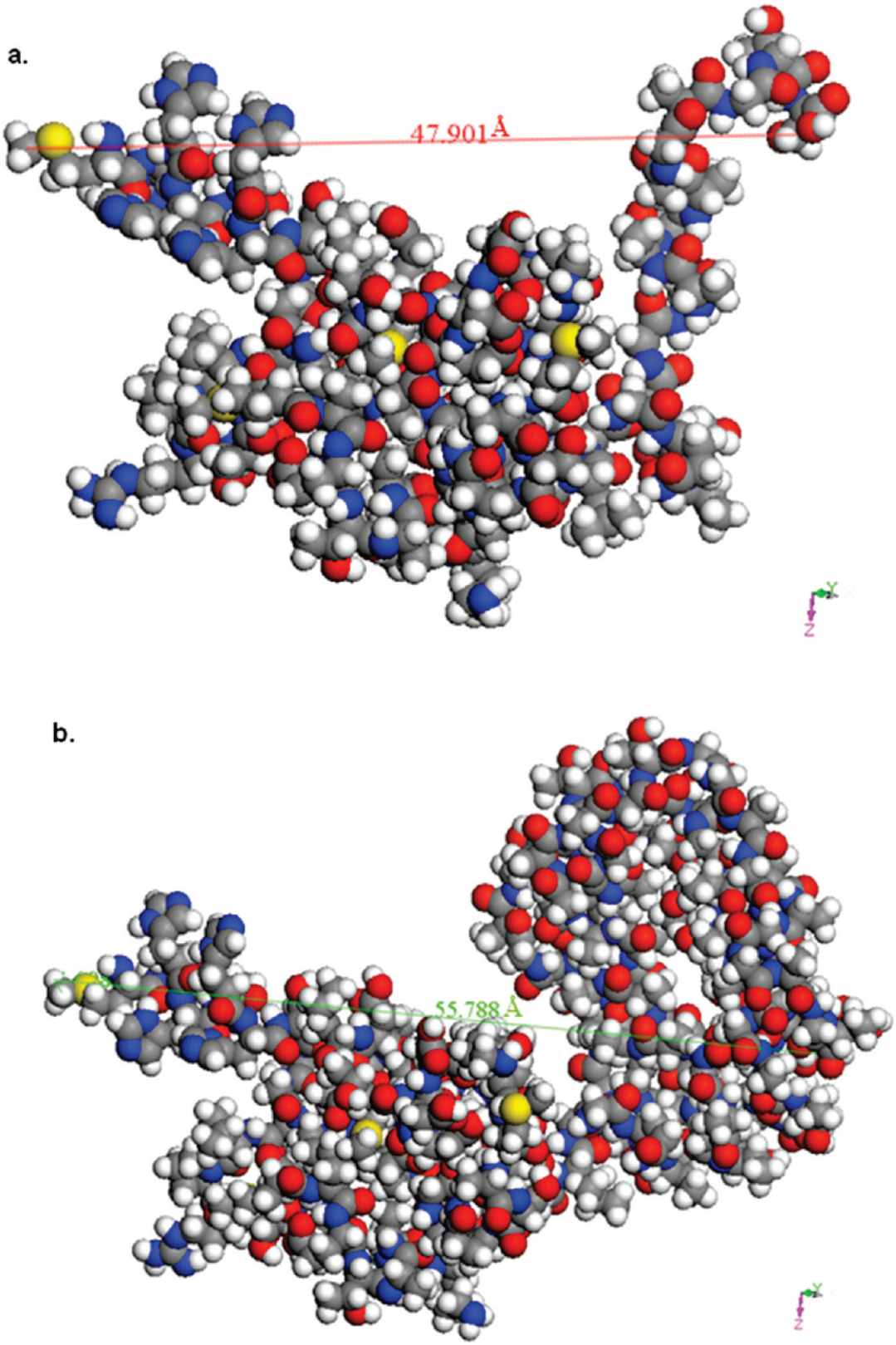

Figure 8. Molecular modeling of HBA (a) and HBA_6 (b). The end-to-end distances are as shown.

compositions. A smooth film is formed for samples with lower numbers of hydrophobic repeats (HBA, HBA_2) (Figures 5a and 6a) at lower pressure in comparison to HBA_6 (Figure 7a). In the case of HBA, the hydrophobic domains start to segregate at medium surface pressures (4 mN/m) with the appearance of discs, whereas at high pressures loose domains spread farther from each other as represented by circular domains (Figure 5b,c). The densely packed feature of HBA_6 at elevated surface pressure is due to sufficient repulsive forces at the interface. From literature, polyalanine units form β-sheets;[36,37] the intramolecular forces are greater, leading to the formation of hairpin-like orientation. This in turn results in closely packed aggregates with each another

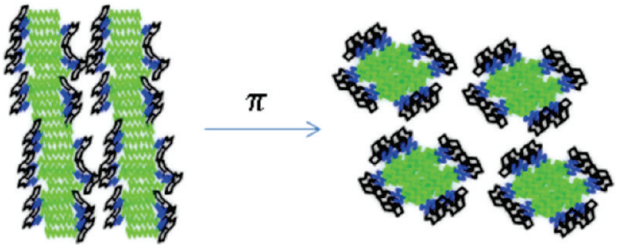

Figure 9. Formation of circular domains from rod-like features for HBA_6. As the pressure increases, the hydrophilic regions (block B) are exposed maximally to water. On further compression, these domains become submerged in the water subphase, inducing aggregation of the hydrophobic block A domains. Green: block A (hydrophobic); blue: block B (hydrophilic).

leading to the formation of circular discs in a compact area (Figure 7c). A schematic representation of block copolymers at higher surface pressure is illustrated in Scheme 2.

HBA_6 forms rod-like patterns at medium surface pressure (Figure 7b). The formation of rod-like structures can be understood in terms of the packing parameter[52] for low molecular weight surfactants. If the hydrophobic chains increase in the spherical micelles, the area occupied by the block copolymer at the core−shell interface increases. Transition to rod shape occurs when the interfacial area per molecule of the spherical micelle exceeds the limit with increasing hydrophobic chain length. As the surface pressure increases, intramolecular forces predominate in the A block and result in a smaller area occupied by them. As a result, spherical micelles become unstable and morphology with smaller curvature, i.e., rod-like, is preferred. Further compression led to rod structures coalescing to circular micelles (Figure 9). Rigid A blocks form a shell whose properties are determined by the bending energy. There is competition between the elastic bending energy and stretching energy resulting in spontaneous curvature and stabilization of the spherical micelles.[4]

3D molecular model of HBA and HBA_6 was applied to compare the orientation of polyalanine segments and total length of the molecules (Figure 8). The chain end-to-end distance was determined as 4.8 and 5.6 nm, respectively. The film thickness measured by AFM was less than that found by modeling, confirming monolayers were formed. Also, HBA_6 forms densely packed structures and appears to form pancake-like 2D morphology, as determined from AFM. By comparing the thickness of the monolayer obtained for HBA_6 and the model, the values are in good agreement, indicating the hydrophobic A blocks are held close by van der Waals forces; hence, they face away from B block.

Conclusions

The ability of novel class of spider silk-like block copolymers to form ordered domain structures at the air−water and air−solid interfaces was investigated. Assembly at the air−water interface was dependent on the number of repeats of polyalanine. Aggregation behavior was investigated at the air−water interface using $\pi-A$ isotherms. All of the protein constructs formed stable monolayer films, with negligible hysteresis based on compression−decompression cycles and diverse surface morphologies as observed by AFM. Loose circular domains were observed for HBA. The structural organization changed as the content of hydrophobic repeats increased. The transitions with HBA_6 involved a change in morphology from circular micelles to rod-like structures, and at higher pressures, to densely packed circular structures. Structure organizational trends concluded from spider silk-like block copolymers brings forth key observations: (a) the number of polyalanine repeats influences the assembly mechanism at the interface, (b) formation of aggregates for HBA_6 at the interface suggests a high propensity to form β-sheets[29] which is confirmed by FTIR, and (c) the Langmuir−Blodgett approach to thin silk films may prove useful in gaining insight into structural changes related to sequence variants. Observed architecture of these thin films can be potential candidates for micro- and nanopatterning, controlled release devices, and biosensors where control of β-sheet in films is necessary. Future interest may also lie whether such films will provide dynamic control over monolayer porosity and surface properties ranging from antifouling to bioscaffolds and tissue engineering applications.

Acknowledgment. We thank the AFOSR and the NSF for financial support.